INTERNATIONAL JOURNAL FOR NUMERICAL AND ANALYTICAL METHODS IN GEOMECHANICS, VOL. 18, 121–131 (1994)

SHORT COMMUNICATIONS

ELASTIC STRESS WAVES IN ROCKBOLTS SUBJECT TO IMPACT LOADING

XIAOPING YI AND PETER K. KAISER

Geomechanics Research Center, Laurentian University, Sudbury, Ontario, P3E 2C6, Canada

SUMMARY

Due to rock bursting or blasting, violent rock ejections can occur. In underground excavations, rockbolts are often used to retain rock blocks that otherwise would be ejected. Employing the stress wave approach, general formulae are derived to compute the elastic stress waves in rockbolts subject to rock block impact loading. Weight-drop tests on steel rods, simulating impact loading of rockbolts, were performed, and a reasonable agreement is found between theoretical predictions and experimental results. The elastic stress wave in an impact loaded steel rod consists of a rider wave and a lower-frequency carrier wave. With the same drop height, the carrier wave becomes more sinusoidal as the mass ratio of steel rod to drop weight is decreased.

INTRODUCTION

Ejection of rocks are often observed during blasting close to free surfaces and during rockbursts in deep hard rock underground mines.[1,2] If rockbolts are used for rock support, they are subject to impact loading by the ejected rock blocks. Wagner[3] used this rock block ejection model to determine support requirements for rockburst conditions in South African gold mines. Yi and Kaiser[4] found that rock blocks can be ejected by both high- and low-frequency seismic waves. Hedley and Whitton[5] reported failures of mechanical bolts during rockbursts at Quirk Mine, Elliot Lake, Canada. This work aims at studying the dynamic response of simulated mechanical bolts subject to axial impact loading.

For the rock block ejection model, formulae for determining the stress wave in a firmly anchored mechanical rockbolt are derived, and stress versus time relationships or stress waves are obtained from step-by-step calculations employing a computer program. Laboratory tests on steel rods loaded by steel drop weights are performed, and comparisons are then made between analytical predictions and experimental results.

STRESS WAVE ANALYSIS

Successive wave sources

The impact loading of a rockbolt in the rock block ejection model is modelled as shown in Figure 1. The top end of the steel rod is fixed to the competent rockmass and the bearing plate at the bottom end accepts the impact of an ejected rock block called the drop weight. This rock

CCC 0363–9061/94/020121–11

Received 21 October 1992
Revised 27 July 1993

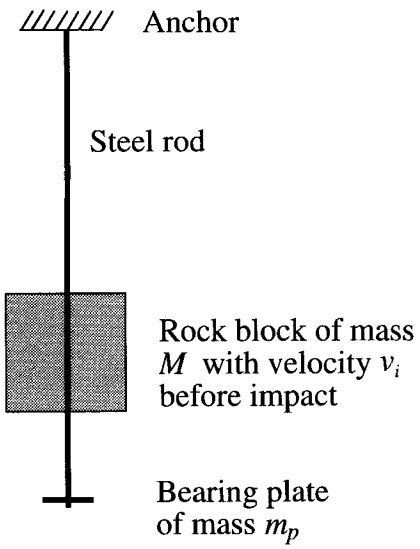

Figure 1. Mechanical model for a mechanically anchored rockbolt loaded by an ejected rock block

block may also be composed of fractured rocks ejected as an entity. Suppose a drop weight of mass M impacts on the bearing plate at an initial velocity of v_i and the two rigid solids (weight and plate) move downwards together. The initial velocity of the bottom plate v_0 immediately after the impact is obtained as follows by employing the law of momentum conservation: $v_0 = v_i M(M + m_p)^{-1}$, with m_p being the mass of the bearing plate. The initial dynamic peak stress in the steel rod at time zero σ_0 is therefore[6] $\sigma_0 = \rho c v_0$, with ρ and c being the density and bar wave propagation velocity of the steel rod, respectively. In the following analysis, the thickness of the rock block is assumed to be very small compared to the length of the steel rod, i.e. the wave propagation in the rock block is ignored.

Immediately after the impact, a stress wave, with the initial stress of σ_0, is generated at the bottom plate and propagates upwards. This wave source is reflected at the fixed top end of the steel rod and then propagates downwards. At a time t_0 (a time variable), after the impact but before the first reflection at the bottom plate, we have the following equation for the equilibrium of the bottom plate and the weight by Newton's second law:

$$-(M + m_p)\frac{dv}{dt_0} = F^{(0)}_{(t_0)} = A\sigma - (M + m_p)g \tag{1}$$

where v is the velocity of the bottom plate (with the weight) at time t_0, σ the stress wave source at the bottom of the steel rod with $\sigma = \rho c v$, g the gravitational acceleration and A the cross-sectional area of steel rod. Here $F^{(0)}_{(t_0)}$ denotes the sum of forces in the steel rod acting on the bottom plate, where the superscript is the reflection number index which indicates, in this instance, *zero* reflection at the bottom plate. From equation (1), the initial stress wave source $\sigma^{(0)}_{(t_0)}$ generated at the bottom plate is obtained as follows:

$$\sigma^{(0)}_{(t_0)} = \exp(\gamma t_0)(I^{(0)}) + \sigma_{st} \quad \text{for } 0 \leqslant t_0 \leqslant 2\tau \tag{2}$$

where $\gamma = -\rho c A(M + m_p)^{-1}$, $\sigma_{st} = (M + m_p)gA^{-1}$ (static stress if the drop weight is not in motion) and $I^{(0)}$ is a stress constant with its superscript being the reflection number index at the bottom plate and τ is the time for a wave to propagate the entire length of the steel rod with

$\tau = Lc^{-1}$. We find $\gamma\tau = -m(M + m_p)^{-1}$. The superscript in $\sigma^{(0)}_{(t_0)}$ again is the reflection number index. Since the initial stress at time zero of the initial wave source is σ_0, the stress constant can be obtained as follows: $I^{(0)} = \sigma_0 - \sigma_{st}$. An equation similar to equation (2) was derived and discussed by Taylor[7] and Kolsky,[8] but the static stress due to the weight of the drop weight was ignored. This static stress must be considered for bolt design where the ejected rock block is large but the ejection velocity is relatively small. As seen from equation (2), the highest value $\sigma^{(0)}_H$ of the initial stress wave source occurs at $t_0 = 0$ and is expressed as $\sigma^{(0)}_H = \sigma_0$, and the corresponding lowest value $\sigma^{(0)}_L$ occurs at $t_0 = 2\tau$ and is expressed as $\sigma^{(0)}_L = \exp(2\gamma\tau) I^{(0)} + \sigma_{st}$.

As stated earlier, the initial stress wave, represented by equation (2), propagates upwards, is reflected at the top end of the steel rod and then propagates downwards. When this wave returns to the bottom plate, it interacts with the bottom plate and a new stress wave source is generated. The old (initial) wave continues its journey up and down the steel rod. Following the same derivation procedure as above, the first stress wave source is obtained as follows:

$$\sigma^{(1)}_{(t_1)} = \exp(\gamma t_1)[I^{(1)} + I^{(0)}(R\gamma t_1)] + \sigma_{st}(1 - R) \quad \text{for } 0 \leqslant t_1 \leqslant 2\tau \tag{3}$$

where t_1 is a new time variable, $I^{(1)}$ the stress constant for the first reflection at the bottom plate, and $R = R_t + R_b$ with R_t and R_b being the reflection coefficients at the top and bottom locations of the steel rod, respectively. R_t equals 1 or 0 for fixed or free top end, and R_b equals 1 or 0 if the bottom plate is fixed on to the steel rod or free to move on it. These reflection coefficients lie between 0 and 1 if the ends are not fixed or if slippage occurs during dynamic loading. Since the downward movement of the bottom plate is continuous, the consecutive stress wave sources are also continuous, i.e. $\sigma^{(1)}_{(t_1=0)} = \sigma^{(0)}_{(t_0=2\tau)}$. The highest value of the first stress wave source $\sigma^{(1)}_H$ occurs at $t_1 = 0$ or $t_0 = 2\tau$, i.e. $\sigma^{(1)}_H = \sigma^{(1)}_{(t_1=0)} = \sigma^{(0)}_{(t_0=2\tau)} = \sigma^{(0)}_L$. In other words, $\sigma^{(1)}_H = \sigma^{(0)}_L = \exp(2\tau\gamma) I^{(0)} + \sigma_{st}$. From equation (3), we obtain $I^{(1)} = \sigma^{(1)}_p - \sigma_{st}(1 - R)$. The stress wave sources expressed in equations (2) and (3) form a continuously declining curve with respect to time.

Further derivations for subsequent reflections at the bottom plate lead to the following general formulae for the determination of the highest and lowest values of successive stress wave sources:

$$\begin{aligned}
\sigma^{(0)}_H &= \sigma_0 \\
\sigma^{(n)}_H &= \exp(2\gamma\tau)\left[I^{(n-1)} + B_1(2R\gamma\tau) + B_2\frac{(2R\gamma\tau)^2}{2!} + \cdots + I^{(0)}\frac{(2R\gamma\tau)^{n-1}}{(n-1)!} \right] + \sigma_{st}(1 - R)^{n-1} \\
I^{(n)} &= \sigma^{(n)}_H - \sigma_{st}(1 - R)^n \\
\sigma^{(n+1)}_H &= \exp(2\gamma\tau)\left[I^{(n)} + (I^{(n-1)} + B_1)(2R\gamma\tau) + (B_1 + B_2)\frac{(2R\gamma\tau)^2}{2!} + \cdots \right. \\
&\qquad \left. + I^{(0)}\frac{(2R\gamma\tau)^n}{n!} \right] + \sigma_{st}(1 - R)^n \\
I^{(n+1)} &= \sigma^{(n+1)}_H - \sigma_{st}(1 - R)^{n+1} \\
\sigma^{(n-1)}_L &= \sigma^{(n)}_H \quad \text{for } n \geqslant 1
\end{aligned} \tag{4}$$

where $\sigma^{(n)}_H$ and $\sigma^{(n)}_L$ are the highest and lowest values of the nth stress wave source after the nth but before the $(n + 1)$th reflection at the bottom plate, $I^{(n)}$ is the corresponding stress constant, and $B_1, B_2, \ldots$ are constants obtained in the step-by-step evaluation following the above formulae.

Stresses at the top and bottom ends of the steel rod

The dynamic stress value at a certain time and location is the superposition of all arriving stress wave sources. We define the peak or valley stress at the nth reflection as the sum of the highest or

lowest values of all (from 0 to nth) arriving stress wave sources. It follows that the peak and valley stresses for the same reflection number have a time span of 2τ, but the valley stress for the nth reflection occurs at the same time as the peak stress for the $(n + 1)$th reflection. For the top end, as an example, at the first reflection the dynamic peak stress is $(1 + R_t)\sigma_0$ or $2\sigma_0$ for $R_t = 1$ and the valley stress is $(1 + R_t)\sigma_H^{(1)}$.

General formulas for the dynamic peak stress at the nth reflection at the top and bottom ends can be obtained as follows:

$$\mathrm{Top}_p^{(n)} = R_b R_t \mathrm{Top}_p^{(n-1)} + (1 + R_t)\sigma_H^{(n-1)} \quad \text{for } n \geqslant 1,$$

and

$$\mathrm{Bottom}_p^{(n)} = R_t \mathrm{Top}_p^{(n)} + \sigma_H^{(n)} \quad \text{for } n \geqslant 0 \tag{5}$$

where $\mathrm{Top}_p^{(n)}$ and $\mathrm{Bottom}_p^{(n)}$ are dynamic peak stresses at the nth reflection at the top and bottom ends, respectively, with $\mathrm{Top}_p^{(0)} = 0$. $\sigma_H^{(n)}$ is given by equation (4). Similarly, the dynamic valley stresses $\mathrm{Top}_v^{(n)}$ and $\mathrm{Bottom}_v^{(n)}$ at the nth reflection at the top and bottom ends are expressed as follows:

$$\mathrm{Top}_v^{(n)} = R_b R_t \mathrm{Top}_v^{(n-1)} + (1 + R_t)\sigma_H^{(n)} \quad \text{for } n \geqslant 1$$

and

$$\mathrm{Bottom}_v^{(n)} = R_t \mathrm{Top}_v^{(n)} + \sigma_H^{(n+1)} \quad \text{for } n \geqslant 0 \tag{6}$$

with $\mathrm{Top}_v^{(0)} = 0$. The dynamic peak and valley stresses at the top and bottom ends of the steel rod in equations (5) and (6) can be computed as a function of the reflection number index n to obtain a stress wave in a steel rod. Since the stress values for the times between two consecutive reflection numbers have not been obtained, straight lines are used as approximations to connect the two points. As seen from equations (4)–(6), the dynamic stress at any reflection number (time) is essentially a function of the initial velocity of the bottom plate v_0 and the mass ratio of the steel rod to the drop weight (represented by $\gamma\tau$). Taylor[7] derived manually the stresses $\mathrm{Top}_p^{(n)}$, $\mathrm{Top}_v^{(n)}$, $\mathrm{Bottom}_p^{(n)}$ and $\mathrm{Bottom}_v^{(n)}$ for up to the second reflection at the bottom plate ($n \leqslant 2$), but, general formulas were not obtained for computer programming.

Numerical examples

Equations (4)–(6) have been coded into a computer program which calculates the stress at consecutive reflection numbers representing the time. Figure 2(a) shows the theoretical stress waves for a weight-drop test. The input parameters are chosen as follows: the reflection coefficients at the top (R_t) and the bottom (R_b) of the steel rod are both 1·0; the density (ρ) and the bar wave velocity (c) of the steel rod are 7750 kg m^{-3} and 5·110 km s^{-1}, respectively; the diameter and the length of the steel rod (L) are 6·35 mm and 2·245 m; the mass of drop weight (M) and the drop height are 2·860 kg and 0·5 m; the mass of the bearing plate (m_p) is 0·144 kg and the gravitational acceleration (g) is 9·8 m s^{-2}.

As seen, a wave is a superposition of a sinusoidal 'carrier wave' and a higher frequency 'rider wave' at both top and bottom positions of the steel rod. The time span between two adjacent peaks of a rider wave is the time span between two adjacent reflection numbers, i.e. twice the time for a wave to propagate the length of the steel rod ($2Lc^{-1}$). This time span is calculated to be 879 μs, and the rise time for an individual peak is zero as assumed. Parametric studies[9] have shown that, for the same drop weight but for different drop heights, stress waves have identical shapes but different stress amplitudes. For the same drop height but for increased mass of

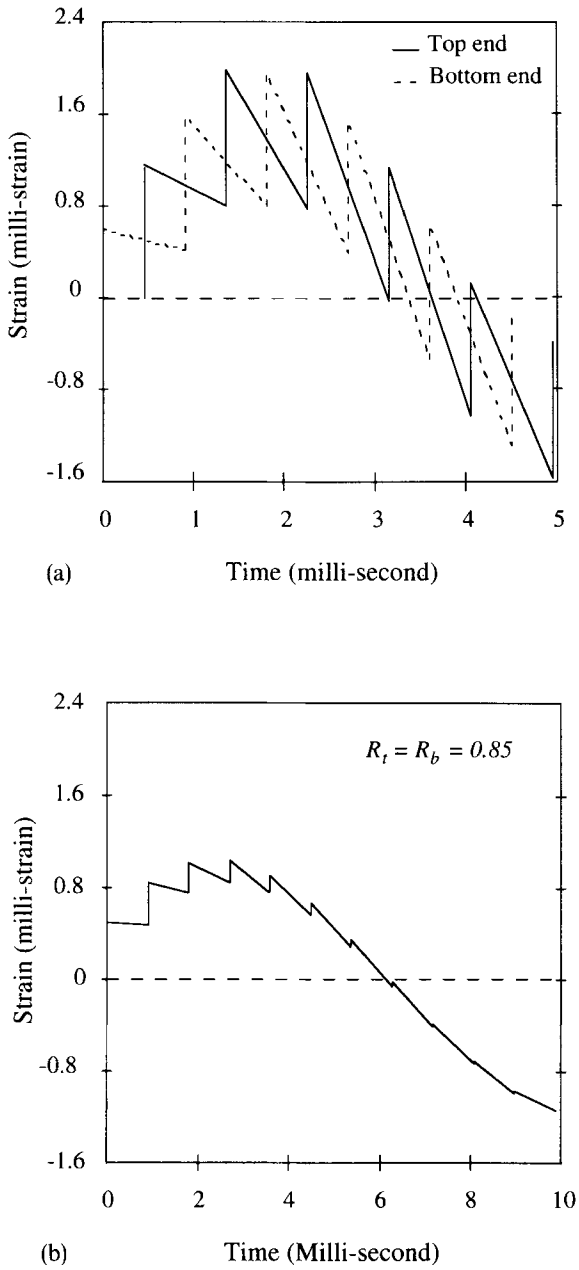

Figure 2. Theoretical strain waves for a drop-weight of 2·86 kg and a height of 0·5 m, assuming (a) complete wave reflections and (b) reflection coefficients of 0·85 for the top and bottom ends of steel rod

a weight, the carrier wave becomes more sinusoidal and the rider wave becomes less pronounced compared to the carrier wave. It must be recognized that if the steel rod is pretensioned, as is the case for a mechanical bolt used in mines, the strain waves in Figure 2(a) must be shifted upwards by an constant equal to the pretension strain.

In order to demonstrate the effect of the reflection coefficient R, the same input parameters as chosen above are utilized except for the assumption of $R_b = R_t = 0{\cdot}85$ which represents partial wave source reflections. The theoretical strain wave at the bottom of the steel rod is shown in Figure 2(b). The amplitude of the wave is substantially reduced and the peaks of the rider wave become smaller with time. This phenomenon was observed in tests employing heavier drop weights.[9] Therefore, the bolt anchor should be allowed to slip under impact loading to reduce dynamic stress in the bolt shank.

EXPERIMENTS

Experimental technique

The experimental set-up is shown schematically in Figure 3. The tests aimed at studying strain waves in steel rods loaded by steel weights dropped from various heights. It must be recognized that this test program is a first step toward understanding rockbolt performance under impact loading, and *in situ* monitoring for seismic and blast loading will be carried out later. The top end of a steel rod was clamped to a concrete beam in the ceiling by using a clamp fixture to simulate an anchored mechanical bolt. A small metal plate having dimensions of 80 mm × 37 mm × 6 mm (thickness) was used to transfer the impact load to the rod, and the plate was fixed to the bottom end of the rod with two nuts (one above and another underneath the plate). A steel tube was employed to protect the steel rod from any bending during weight dropping. The steel rod was 6·35 mm in diameter and 2·44 m in length, but its effective length between the top clamp and the bearing plate was 2·245 m. Six steel weights were numbered as 'weight No. 1–6' with masses of 0·5, 1·004, 2·032, 2·860, 3·572 and 17·723 kg, respectively. The heights of these drop weights varied betwen 76 and 150 mm, much less than the length of the steel rod. Three drop heights were numbered as 'height No. 1, 2 and 3' which measured 0·1, 0·5 and 1·4 m, respectively. Each test with a given combination of weight and height was repeated three times to provide representative data.

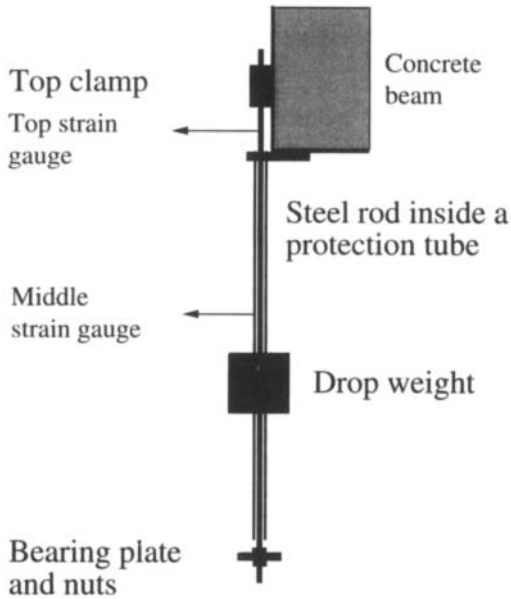

Figure 3. Experimental set-up for weight-drop tests

Two strain gauges were used to measure the strain waves in the steel rod. They were of type EP-08-125AD-120 (with a gauge factor of 2·06 ± 0·5 per cent) from Measurements Group Inc., Raleigh, North Carolina. A strain gauge was 1·57 mm in length (aligned with the direction of strain) and 3·05 mm in width and had a strain limit of 20 per cent. The glue for the strain gauges was a M-Bond GA-2 Kit (Resin GA-2 and Hardener 10-A) with a strain limit of 10–15 per cent. In the trials, two strain gauges were mounted on diametrically opposed sides of the steel rod at the top location, and it was found that bending could be ignored, particularly for the first half period of the strain wave. Because of the need to install additional strain gauges at a lower position in subsequent testing, only one strain gauge was installed at each location in order to maintain a high sampling rate. The top strain gauge was located immediately under the top clamp and the middle strain gauge was 1·16 m below the top strain gauge, i.e. near the midpoint of the steel rod. A strain gauge conditioner (2100 system) from the same company was used to amplify the strain signals and a computer data acquisition system was used to display and store the strain waves. The system included a Compaq 286 computer, a data acquisition card and data processing software from RC Electronics. The maximum sampling rate of the system with two channels in use was 0·5 MHz or 2 μs per sample.

Experimental results

Figure 4 shows the entire strain waves recorded by the top and middle strain gauges for a test with drop weight No. 4 and height No. 2 (test No. 4-2). In agreement with a theoretical stress wave, a high-frequency rider wave rides on a low-frequency carrier wave for both strain gauges. However, it was observed that the drop weight rebounded after the first impact. The latter portion of a strain wave beyond its first half period was the superposition of waves from the first impact and those from subsequent rebounds, but this latter portion always had a much smaller amplitude. Therefore, the assumption that the drop weight moves together with the bearing plate

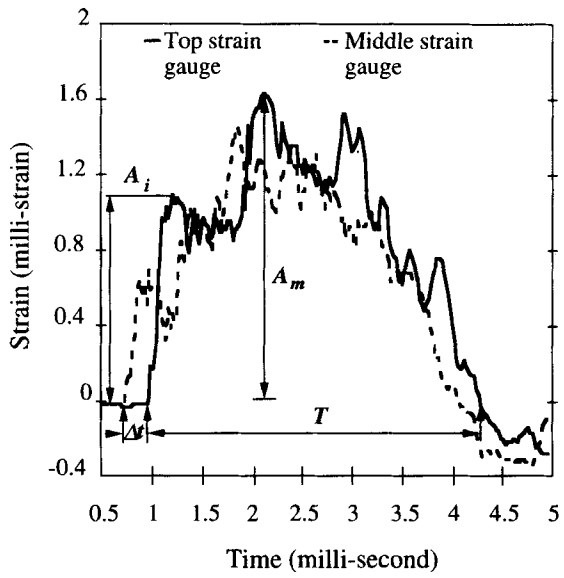

Figure 4. Strain waves from one of three tests for No. 4-2 with the same drop weight and height as those assumed in the theoretical prediction (Figure 2(a))

is realistic for the first half period of time, and the following analyses focus on this portion of the wave. For the characterization of the recorded waves, the following parameters for the first half period of wave are defined: the amplitude A_m, the half period T, the initial peak A_i and the time lag between waves from two strain gauges Δt. The time span between the first two peaks of the rider wave for the top strain gauge is about 900 μs which is in good agreement with the theoretical value of 879 μs. Tests performed with different combinations of drop weights and heights showed that for the same weight, the waveforms for different heights had similar shapes but different amplitudes. For the same drop height but with a heavier weight, the carrier wave became more sinusoidal and the rider wave relatively less prominent.[9] This qualitative statement agrees with the theoretical result.

The time lag parameter was measured for one of the three repeated tests for each combination of drop weight and height, and the mean and standard deviation was $\Delta t = 227 \pm 1$ μs (11 data). Having measured the distance between the two strain gauges, the wave velocity is determined to be $c = 5{\cdot}11$ km s^{-1}. The strain waves can be transformed into stress waves by multiplying strain values by the dynamic Young's modulus E_d of the steel rod. It can be determined from the following formula:[6] $E_d = c^2\rho = 202$ GPa, with a density of $\rho = 7750$ kg m^{-3} for the steel rod. The first and second peaks of the rider wave for the middle strain gauge are spaced at about 0·45 ms (Figure 4) which is only half that for the top strain gauge and corresponds to a propagation distance of 2·3 m. The first peak is caused by the impact of the drop weight and the second is its reflected image from the top clamp. The strain wave from the middle strain gauge appeared to be smoother than from the top strain gauge because the rider wave had smaller peaks and were more closely spaced.

QUANTITATIVE COMPARISONS BETWEEN PREDICTIONS AND MEASUREMENTS

Theoretical values for wave amplitude A_m, half period T and initial peak amplitude A_i are calculated using the computer program mentioned previously for all combinations of drop

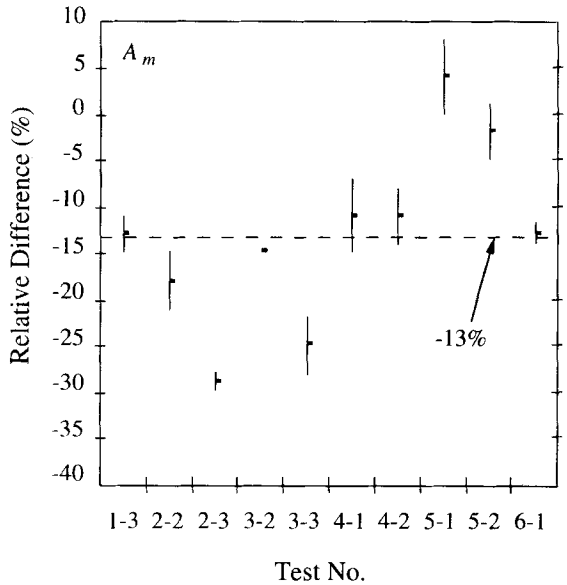

Figure 5(a)

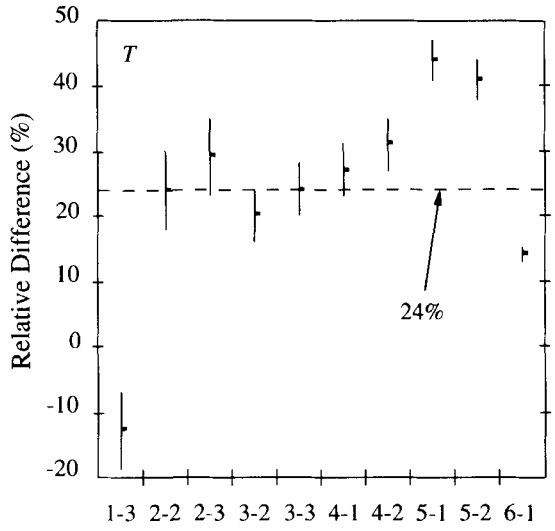

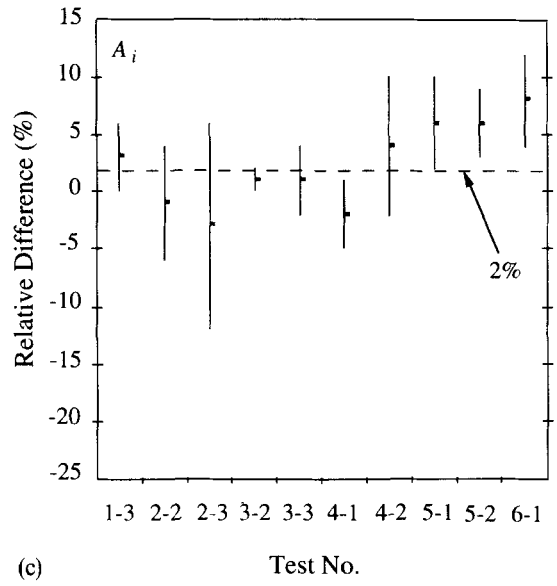

Figure 5. Relative differences in (a) wave amplitude A_m, (b) half period T and (c) initial peak amplitude A_i between measured and predicted values with the dashed line indicating the average for all mean values

weights and heights employed in the laboratory testing program. It is assumed that the top end of a steel rod is fixed to the concrete beam, and the bottom plate fixed to the bottom end of the steel rod. Relative differences between experimental values (from the top strain gauge) and theoretical values (evaluated for the top end of the steel rod) are calculated and plotted in Figures 5(a)–5(c). The relative difference is the difference between experimental (mean $\pm$ standard deviation) and theoretical values divided by the theoretical value. It should be zero for a perfect fit. A test number

on the horizontal axis is denoted by two digits separated by a hyphen. It represents a group of three repetitive tests for the same drop weight and height indicated by the first and the second digit, respectively.

The relative differences in the amplitude of the first half period of the wave (A_m) shown in Figure 5(a) vary from -29 ± 1 per cent (test No. 2-3) to 4 ± 4 per cent (test No. 5-1) with an average of -13 per cent for all mean values. The relative differences in the half period T shown in Figure 5(b) vary from negative to positive values with an average of 24 per cent for all mean values. The relative differences in the initial peak amplitude (A_i) are essentially insignificant with an average of 2 per cent for all mean values. These relative differences are considered to be quite small. They may have resulted from steel rod bending due to eccentricity of loading because of the following imperfections in the experimental technique: (i) the steel rod was not perfectly straight and vertical and the bottom plate was not perfectly horizontal; (ii) the steel tube was not perfectly concentric with the steel rod and (iii) errors exist in picking the values of the three parameters from experimental curves (Figure 4). Some bending of steel rods was detected using two strain gauges installed on diametrically opposed sides of a different steel rod.[9] Hence, the differences between measurements and predictions do not seem to be of a fundamental nature, and it may be concluded that the stress wave analysis provides a reasonable approximation for laboratory test data.

DISCUSSION AND CONCLUSIONS

The Geomechanics Research Center of Laurentian University in Sudbury has undertaken to monitor rockbolt performance under blast or seismic loading in underground mines. The analytical results obtained above are currently applied to the design of the experiments and they will facilitate the interpretation of measured stress waves. The present analysis showed that the stress wave may be reduced if partial wave transmission from the rockbolt to the competent rockmass is achieved or if the anchor of a rockbolt slides. Therefore, sliding mechanisms, including but not limited to sliding nuts for mechanical bolts and debonding for fully grouted rockbolts, should be exploited in designing and installing rockbolts.

The following conclusions can be made from the analyses and experiments. The stress wave analysis provides a reasonable estimate for the measured elastic stress waves in weight-drop tests on steel rods. An elastic stress wave consists of a rider wave and a lower-frequency carrier wave. With the same drop height, the carrier wave becomes more sinusoidal and the rider wave less prominent as the mass ratio of steel rod to drop weight is decreased. This analytical method may be applied to estimating stress waves in mechanical rockbolts subject to impact loading during rockbursts and blasting.

ACKNOWLEDGEMENTS

Laboratory assistance from S. Maloney and G. McDowell and financial support provided by the Natural Sciences and Engineering Research Council (NSERC) of Canada are gratefully acknowledged.

REFERENCES

1. W. D. Ortlepp, 'Invited lecture: the design of support for the containment of rockburst damage in tunnels—an engineering approach', in P. K. Kaiser and D. McCreath (eds), *Proc. Int. Symp. on Rock Support*, Sudbury, Ontario Canada, Balkema (Rotterdam), 1992, pp. 593–610.
2. Ontario Ministry of Labor, 'Interpretation 34a of regulation 694', *Occupational Health and Safety Act and Regulations for Mines and Mining Plants*, Occupational Health and Safety Division, 400 University Avenue, Toronto, Canada, M7A 1T7, 1990.

3. H. Wagner, 'Support requirements for rockburst conditions', in N. C. Gay and E. H. Wainwright (eds), *Proc. 1st Int. Symp. on Rockbursts and Seismicity in Mines*, Johannesburg, 1982, SAIMM, 1984, pp. 209–218.
4. X. Yi and P. K. Kaiser, 'Mechanisms of rockmass failure and prevention strategies in rockburst conditions', in R. P. Young (ed), *Proc. 3rd Int. Symp. on Rockbursts and Seismicity in Mines*, August 16–18, Kingston, Canada, 1993, pp. 141–145.
5. D. F. G. Hedley and N. Whitton, 'Performance of bolting systems subject to rockbursts', *CNCRM Symp. on Underground Support Systems*, Canadian Institute of Mining and Metallurgy, September 19–21, 1983.
6. B. G. H. Brady and E. T. Brown, *Rock Mechanics for Underground Mining*, George Allen and Unwin, UK, 1985.
7. G. I. Taylor, 'The testing of materials at high rates of loading–James Forrest Lecture', *J. Inst. Civil Eng.*, **26**, 486–519 (1946).
8. H. Kolsky, *Stress Wave in Solids*, Dover, New York, 1963.
9. X. Yi, Dynamic response and design of support elements in rockburst conditions, *Ph. D. Thesis*, Department of Mining, Queen's University, Kingston, Ontario, Canada, 1993.